

Atlantic-Origin Overflow Water in the East Greenland Current

LISBETH HÅVIK

Geophysical Institute, and Bjerknes Centre for Climate Research, University of Bergen, Bergen, Norway

MATTIA ALMANSI

Department of Earth and Planetary Sciences, The Johns Hopkins University, Baltimore, Maryland

KJETIL VÅGE

Geophysical Institute, and Bjerknes Centre for Climate Research, University of Bergen, Bergen, Norway

THOMAS W. N. HAINE

Department of Earth and Planetary Sciences, The Johns Hopkins University, Baltimore, Maryland

(Manuscript received 24 October 2018, in final form 13 June 2019)


ABSTRACT

Dense water masses transported southward along the east coast of Greenland in the East Greenland Current (EGC) form the largest contribution to the Denmark Strait Overflow. When exiting Denmark Strait these dense water masses sink to depth and feed the deep circulation in the North Atlantic. Based on one year of mooring observations upstream of Denmark Strait and historical hydrographic profiles between Fram Strait and Denmark Strait, we find that a large part (75%) of the overflow water ($\sigma_\theta \geq 27.8 \text{ kg m}^{-3}$) transported by the EGC is of Atlantic origin (potential temperature $\theta > 0^\circ\text{C}$). The along-stream changes in temperature of the Atlantic-origin Water are moderate north of 69°N at the northern end of Blossville basin, but southward from this point the temperature decreases more rapidly. We hypothesize that this enhanced modification is related to the bifurcation of the EGC taking place close to 69°N into the shelfbreak EGC and the separated EGC. This is associated with enhanced eddy activity and strong water mass modification reducing the intermediate temperature and salinity maxima of the Atlantic-origin Water. During periods with a large (small) degree of modification the separated current is strong (weak). Output from a high-resolution numerical model supports our hypothesis and reveals that large eddy activity is associated with an offshore shift of the surface freshwater layer that characterizes the Greenland shelf. The intensity of the eddy activity regulates the density and the hydrographic properties of the Denmark Strait Overflow Water transported by the EGC system.

1. Introduction

The circulation in and north of Denmark Strait is complex and exhibits high temporal and spatial variability (e.g., Våge et al. 2013; Harden et al. 2016; Behrens et al. 2017; von Appen et al. 2017; Håvik et al. 2017b; Almansi et al. 2017). The strongest current flowing into Denmark Strait is the shelfbreak East Greenland Current (EGC; Fig. 1; Våge et al. 2013;

Harden et al. 2016). This current originates north of Fram Strait and continues southward along the east Greenland shelf toward the southern tip of Greenland. At the northern end of Blossville basin the shelfbreak EGC bifurcates and a second branch, the separated EGC, flows southward along the base of the Iceland slope (Fig. 1). Near the Kögur transect (Fig. 1) the separated EGC partly merges with the North Icelandic Jet (NIJ) flowing southwestward from the Iceland Sea, and the combined flow follows the deep part of the

 Denotes content that is immediately available upon publication as open access.

Corresponding author: Lisbeth Håvik, lisbeth.havik@uib.no



This article is licensed under a [Creative Commons Attribution 4.0 license](http://creativecommons.org/licenses/by/4.0/) (<http://creativecommons.org/licenses/by/4.0/>).

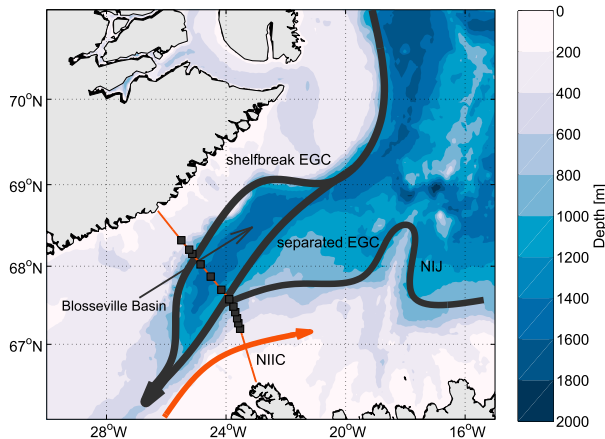


FIG. 1. Schematic overview of the currents flowing across the Kögur mooring array marked by the orange line between Greenland and Iceland. The abbreviations are EGC = East Greenland Current, NIJ = North Icelandic Jet, and NIIC = North Icelandic Irminger Current.

Iceland slope toward Denmark Strait (Harden et al. 2016). The two EGC branches and the NIJ are the primary pathways of both light surface water and dense overflow water from the Nordic Seas through Denmark Strait to the North Atlantic.

The bulk of the freshwater in the western Nordic Seas is situated on the east Greenland shelf and the southward transport largely takes place in the shelfbreak EGC (Haine et al. 2015; de Steur et al. 2017), although the transport on the shelf may be substantial (Håvik et al. 2017a). Some freshwater is also diverted east into the Greenland and Iceland Seas (Bourke et al. 1992; Jónsson 1992; Macrandar et al. 2014). Both of these basins are known for deep and intermediate convection (Våge et al. 2015; Latarius and Quadfasel 2016; Brakstad et al. 2019; Våge et al. 2018), and the transformed water masses contribute to the dense overflows from the Nordic Seas (e.g., Eldevik et al. 2009). The presence of a fresh surface layer, however, can inhibit convection and subsequently alter the properties of the overflow water (Brakstad et al. 2019).

The dense water mass passing through Denmark Strait [Denmark Strait Overflow Water (DSOW)] accounts for approximately half of the overflow water export from the Nordic Seas to the North Atlantic (Hansen et al. 2016; Jochumsen et al. 2017; Østerhus et al. 2019). These water masses are denser than the surrounding water in the North Atlantic and sink to the abyss where they contribute to the deep western boundary current and the Atlantic meridional overturning circulation (Lozier et al. 2017). The DSOW is a mixture of water masses and its hydrographic properties depend on the relative contributions from each source region and the along-stream

modification in the currents transporting it toward Denmark Strait (Jónsson 1999; Jeansson et al. 2008; Mastropole et al. 2017). DSOW is typically defined by having a potential density $\sigma_\theta \geq 27.8 \text{ kg m}^{-3}$ (e.g., Dickson and Brown 1994), and Harden et al. (2016) estimate that two-thirds of it is transported toward Denmark Strait by the EGC and that the remaining portion is supplied by the NIJ.

A substantial westward flux of Atlantic Water from the West Spitsbergen Current takes place in Fram Strait (de Steur et al. 2014; Hattermann et al. 2016; von Appen et al. 2016; Håvik et al. 2017a). Before entering the EGC, heat and salt fluxes have modified the hydrographic properties of the Atlantic Water during the transit northward through the eastern Nordic Seas. The modified Atlantic Water merges with the EGC below the fresh Polar Surface Water (PSW) and comprises a large portion of the DSOW (Mauritzen 1996; Eldevik et al. 2009). In the EGC the modified Atlantic Water can typically be recognized by an intermediate temperature and salinity maximum. We use the term Atlantic-origin Water for all intermediate water masses with a potential temperature $> 0^\circ\text{C}$ (Våge et al. 2011). This is mostly recirculated Atlantic Water from Fram Strait, although some portion is Atlantic Water which has circulated around the Arctic Ocean (Buch et al. 1996; Mauritzen 1996; Rudels et al. 2002, 2005). En route from Fram Strait to Denmark Strait the intermediate water masses of the EGC are modified through isopycnal mixing with the water masses in the interior basins (Strass et al. 1993), and through direct contact with the atmosphere (Våge et al. 2018). North of Denmark Strait the EGC can be distinguished from the NIJ by its hydrographic properties as the NIJ transports a water mass with a lower salinity and temperature than the Atlantic-origin Water (typically $\theta < 0^\circ\text{C}$ and $S < 34.9$; Harden et al. 2016).

The extent to which overflow waters are modified during transit to the Denmark Strait influences both the hydrographic properties of the overflow layer and potentially also its density. Ultimately, the density of the DSOW may influence the large-scale circulation of the North Atlantic. It is of interest to understand where and how this modification takes place. We focus on the modification of the Atlantic-origin Water in the EGC based on historical hydrographic profiles of temperature and salinity between Fram Strait and Denmark Strait as well as a year of hydrographic and velocity measurements obtained from moorings along the Kögur transect (Fig. 1) in 2011–12. In particular, the year-long dataset from the east Greenland shelf and slope cover a historically sparsely sampled part of the EGC. In addition, we show results from a high-resolution numerical model

in and north of Denmark Strait. We connect the modification of the Atlantic-origin Water and the kinematic structure of the EGC system north of Denmark Strait and discuss some implications for the distribution and transport of both light surface water and the dense DSOW.

2. Data and methods

a. The Kögur mooring array

From September 2011 to August 2012 an array consisting of 12 moorings sampled the two EGC branches and the NIJ along the Kögur transect north of Denmark Strait (Fig. 1). The moorings spanned from the outer east Greenland shelf to the Iceland shelf break, and were equipped with various instruments measuring both hydrography and velocity. Point measurements of velocity were obtained by recording current meters (RCMs) and Aquadopp current meters, and profiles of velocity by acoustic Doppler current profilers (ADCPs). The hydrography was sampled by MicroCats and coastal moored profilers. The data return was excellent, and most of the instruments gave 11 full months of data. Both the hydrographic and the velocity data were interpolated onto a regular grid using a Laplacian-spline interpolator with a spatial resolution of 8 km in the horizontal and 50 m in the vertical, and a temporal resolution of 8 h. We note that the hydrographic data was extrapolated between 100 and 50 m. See Harden et al. (2016) for a full description of the data, the methods applied in the gridding, and a discussion of the error sources.

b. Historical hydrographic profiles

We use a selection of historical conductivity, temperature, and depth (CTD) data from the western Nordic Seas between 67° and 78°N from 1980 to 2014 (Våge et al. 2015), to investigate the hydrographic properties of the Atlantic-origin Water in the shelfbreak EGC upstream of Denmark Strait. The profiles were selected based on a few specific criteria. First, all profiles had to be located within a distance of 0.2° from the 700-m isobath on the east Greenland slope. This is a typical isobath over which the shelfbreak EGC is located (Håvik et al. 2017b) but due to the steepness of the slope the exact choice of isobath did not influence the selection considerably. Since we focus on the Atlantic-origin Water all profiles with only subzero temperature were omitted. In addition we required that the intermediate ($\sigma_\theta > 27.8 \text{ kg m}^{-3}$) Atlantic-origin layer was thicker than 50 m and that the profiles reached the depth of the temperature maximum, that is, where the temperature gradient changed sign. Second, the profiles

were interpolated onto a regular depth vector with 10-m resolution and low-pass filtered with a 50-m Hann window to reduce noise. Last, a few profiles with spurious salinity data were removed manually. Based on these criteria we obtained 380 CTD profiles sampling the Atlantic-origin layer along the east Greenland shelf between Fram Strait and Denmark Strait. Almost all of the profiles were obtained between June and November (361 out of 380 profiles), with no systematic change over the 35-yr period.

c. Numerical circulation model

We use a high-resolution numerical circulation model to investigate the role of mesoscale eddies along the path of the shelfbreak EGC between Fram Strait and Denmark Strait. The dynamics were simulated using the Massachusetts Institute of Technology General Circulation Model (MITgcm; Marshall et al. 1997). This configuration is publicly available on the Johns Hopkins University SciServer system (<http://www.sciserver.org/integration/oceanography/>). The model domain was centered on Denmark Strait and included the entire Iceland Sea to the north. The horizontal resolution was 2 km over the center of the domain (between 60° and 71°N) and decreased toward the boundaries (the minimum resolution was about 4 km at 76°N). The vertical domain is discretized by 216 levels giving a vertical resolution that linearly increases from 1 to 15 m in the upper 120 m and is 15 m thereafter. The model was run for one year (from September 2007 to August 2008) storing the output every 6 h. The model setup was identical to the configuration used and described by Almansi et al. (2017). However, the atmospheric boundary conditions were provided every 3 h using the 15-km resolution regional Arctic System Reanalysis (ASRv2; Bromwich et al. 2018) instead of the global atmospheric reanalysis ERA-Interim (Dee et al. 2011). The spatial resolution of the atmospheric fields plays a major role in controlling the model ocean circulation (Haine et al. 2009), and the model configuration forced by ASRv2 better captured the dynamics associated with barrier winds and katabatic flows (Moore et al. 2016).

The oceanic component was coupled with the MITgcm sea ice model (Losch et al. 2010), using the monthly reanalysis toward an Operational Prediction System for the North Atlantic European Coastal Zones (TOPAZv4; Sakov et al. 2012) to provide the sea ice initial and boundary conditions. A particular effort was made to obtain realistic freshwater forcing which was a key feature of the numerical setup used here. Freshwater from solid ice discharge was distributed along the Greenland coast using a combination of climate models, remote sensing, and terrestrial data (Bamber et al. 2012).

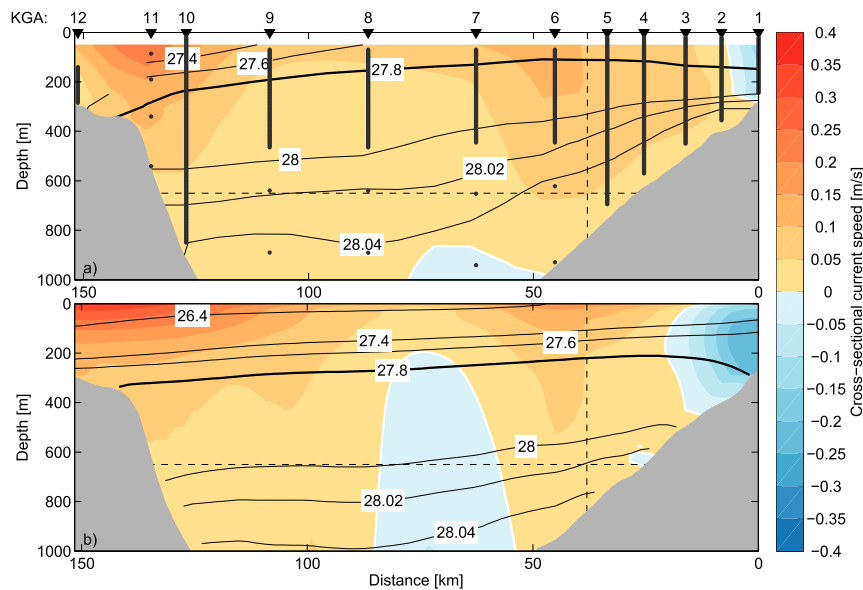


FIG. 2. Comparison of the mean cross-sectional current speed in (a) the mooring observations and (b) the model at Kögur. Positive current speeds are toward the southwest and distance is increasing along the x axis from the easternmost mooring near the Iceland shelf break. On top of (a) the mooring locations are numbered (KGA 1–12), and the measurement levels on each mooring are marked by black dots. A selection of isopycnals is contoured in both panels, and the upper limit of DSOW, the 27.8 kg m^{-3} isopycnal, is marked by the thick black contour. The horizontal dashed line indicates the sill depth at Denmark Strait (650 m), and the vertical dashed lines mark the location where the orientation of the transect changes. The data from the mooring array were interpolated using a Laplacian-spline interpolator (see section 2a), and the data from the model were linearly interpolated in the horizontal.

Furthermore, the daily 1-km Greenland Ice Sheet surface mass balance (Noël et al. 2016) was used to estimate surface runoff.

d. Comparison between model and observations

Almansi et al. (2017) showed that the major currents and water masses observed in Denmark Strait were captured by the model and the simulated velocities compared very well with observations. The hydrographic structure also resembled the observations well, although the overflow temperature in the model was about 1°C too warm. The temperature bias mostly concerns the deep part of the water column, and Almansi et al. (2017) estimated that the magnitude of the density bias was about 0.1 kg m^{-3} . The authors also reported a stronger seasonal cycle than in the observations analyzed by Mastropole et al. (2017) and von Appen et al. (2017).

We compare the model velocity field with observations upstream of Denmark Strait. The mean cross-sectional current speed from the model agrees well with the observations at Kögur (Fig. 2). The strength of the shelfbreak EGC was similar in both cases, although the model exhibited a wider current. On the Iceland slope

the combination of the separated EGC and the NIJ was evident as a surface-intensified current, situated approximately above the 600–800-m isobaths in both the observations and the model. At the upper Iceland slope the negative (northeastward) velocities represented the North Icelandic Irminger Current. The model was generally less dense than the observations, consistent with the biases found in Denmark Strait by Almansi et al. (2017). In addition, the characteristic divergence of isopycnals associated with the NIJ was less pronounced in the model than in the observations (Våge et al. 2011; Harden et al. 2016). Our focus is on the shelfbreak and separated branches of the EGC, and we conclude that the model represents well the kinematic structure of both. We note that the model simulated one year, whereas the observations along the Greenland shelf break were biased toward late summer and spread over 35 years.

3. Atlantic-origin Water in the shelfbreak East Greenland Current at Kögur

Using the same mooring data, Harden et al. (2016) estimated a transport of $1.5 \pm 0.16 \text{ Sv}$ ($1 \text{ Sv} \equiv 10^6 \text{ m}^3 \text{ s}^{-1}$)

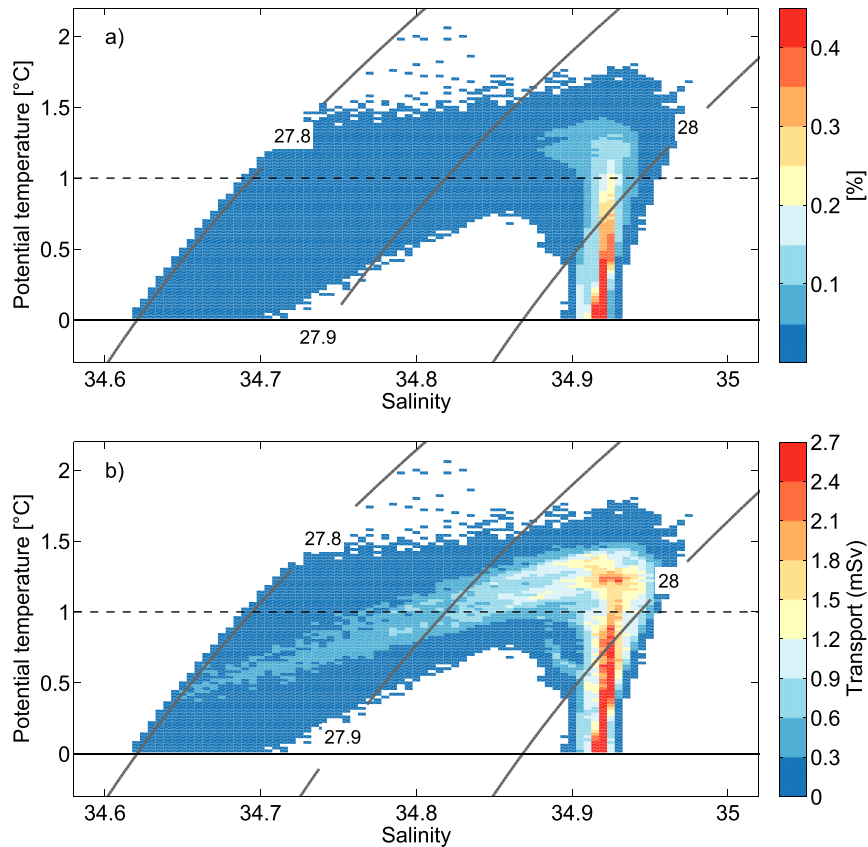


FIG. 3. (a) Occurrence and (b) volume transport of Atlantic-origin Water from September 2011 to August 2012 in the shelfbreak EGC at the Kögur mooring section as a function of temperature and salinity. We only considered water masses with $\sigma_{\theta} \geq 27.8 \text{ kg m}^{-3}$. The water masses were divided by increments of 0.02°C in temperature and 0.005 in salinity. The contours are potential density (kg m^{-3}) and the horizontal dashed lines mark the 1°C isotherm.

of DSOw in the shelfbreak EGC. Of this, we calculated that the Atlantic-origin Water accounted for approximately 75% of the overflow water transport, confirming the results of Mauritzen (1996) and Eldevik et al. (2009) that the main constituent of DSOw is of Atlantic origin. In potential temperature and salinity (θS) space the Atlantic-origin Water with overflow density in the shelfbreak EGC at Kögur spanned a relatively narrow range of hydrographic properties. Most of the water had a temperature below 1°C and a salinity around 34.92 (Fig. 3a). A portion of this water mass, however, had a temperature above 1°C . Although this warmer water mass was less abundant than the colder Atlantic-origin Water, its transport was relatively strong (Fig. 3b). In particular, a water mass with temperature $> 1^{\circ}\text{C}$ appeared to contribute substantially to the transport of DSOw. Based on this we separated the Atlantic-origin Water into a warm mode ($\theta > 1^{\circ}\text{C}$) and a cold mode ($0^{\circ} < \theta < 1^{\circ}\text{C}$). To understand the modification of the Atlantic-origin Water in the shelfbreak EGC north of

the Kögur transect, we examined historical CTD profiles between Fram Strait and Denmark Strait.

4. Atlantic-origin water in the East Greenland Current between Fram Strait and Denmark Strait

We focused on the core properties of the Atlantic-origin Water in the historical profiles and defined this by the intermediate temperature maximum of each profile and its corresponding salinity (Mauritzen 1996; Håvik et al. 2017a). In general, the intermediate temperature maximum decreased from north to south (Fig. 4a), with a corresponding decrease in salinity (Fig. 4b). This is not surprising as the neighboring water masses are of polar and arctic origins, and an exchange with these colder and less saline water masses leads to a reduction in temperature and salinity from Fram Strait to Denmark Strait. In addition, the range of maximum temperatures decreased from north to

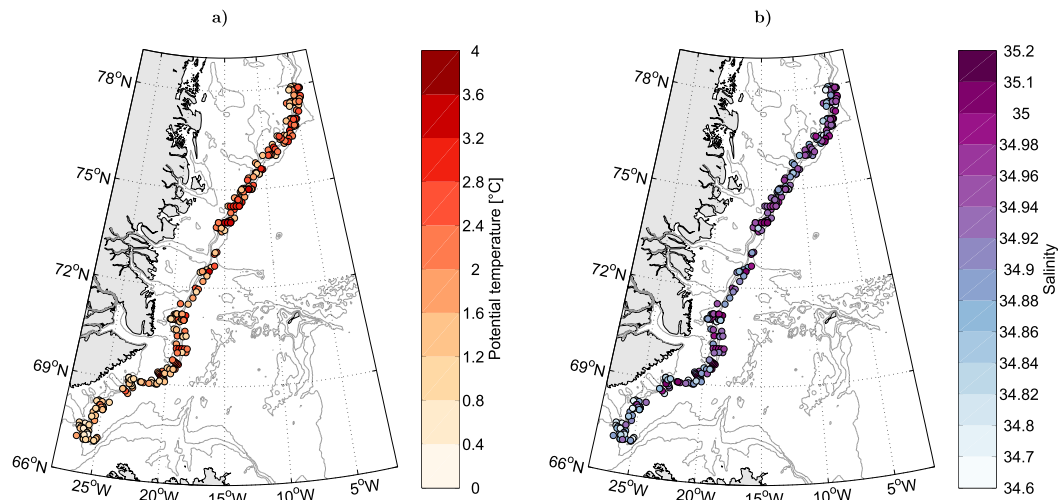


FIG. 4. (a) Maximum temperature and (b) corresponding salinity of the Atlantic-origin layer in the shelfbreak EGC. The gray contours are the 300-, 700-, 1000-, and 2000-m isobaths obtained from the ETOPO2 database.

south, mainly due to a reduction in the warm core temperatures (Fig. 5a).

A linear least squares fit of the temperature maximum of the Atlantic-origin Water from north to south gives an average decrease in temperature of 0.1°C per degree of latitude (Figs. 5a,b). However, the data indicate that the trend is not constant and a change in trend between

68° and 70°N seems probable. To locate a possible breakpoint in the trend we first compared the linear trend of all data, with the trend of the data south of a given latitude (Fig. 5b). We checked for potential breakpoints every 0.5° of latitude and estimated a confidence level for the trends based on a bootstrap method with 1000 times resampling (shading in Fig. 5b).

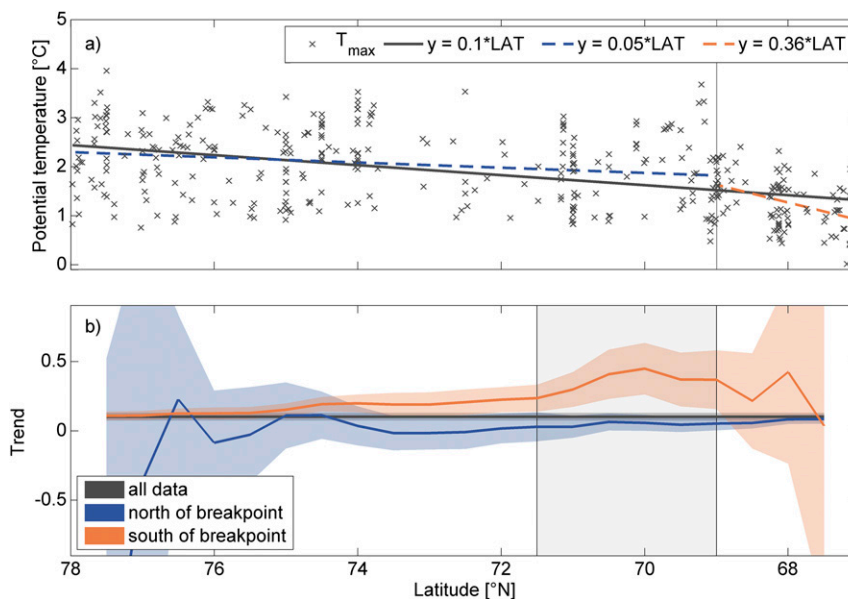


FIG. 5. (a) Scatter of maximum Atlantic-origin Water temperature with latitude. The black trend line indicates a linear fit to all data. The dashed blue line is the linear fit north of a given latitude, and the dashed orange line is the linear fit south of a given latitude. The breakpoint at 69°N is marked by a vertical line (see the text for an explanation of how this was determined). The magnitudes of the trends are indicated in the legend. (b) Trend estimates north (blue) and south (orange) of any given latitude with the 99% confidence interval marked by the colored shading. The average trend of all data is given by the horizontal dark gray line.

The area where the confidence interval of the trend south of the breakpoint and the confidence interval of the trend of all data did not overlap, is where the trends are different ($>99\%$ confidence interval). This method indicated a region of different trends between 69° and 71.5°N marked by the light gray shading in Fig. 5b. For completeness we also present the trend north of any given breakpoint. This was not statistically different from the mean trend of all data at any point.

To pinpoint the location of a breakpoint within the region of different trends we calculated the root-mean-squared error (RMSE) between the data and the estimated trends. The RMSE describes the goodness of a fit, where a lower value indicates a better fit. Within the shaded region of statistically different trends a minimum in RMSE was found at 69°N . Taken together, the results from Fig. 5b and the RMSE values demonstrated the existence of a significant breakpoint near 69°N .

South of the breakpoint the Atlantic-origin Water temperature decreased by 0.36°C per degree of latitude, that is, more than 3 times faster than indicated by the linear fit of the entire dataset. Våge et al. (2013) hypothesized that the EGC bifurcates near 69°N due to the combination of a sharp bend in bathymetry and wind forcing. The bifurcation is likely connected to increased current variability. This was supported by estimates of eddy kinetic energy (EKE) calculated from satellite altimetry, which revealed that this region south of approximately 69°N is a local maximum for eddy activity in the Nordic Seas (Håvik et al. 2017b). An eddy-rich flow is associated with strong velocity shear and effective mixing which can lead to a more rapid modification of hydrographic properties than in more quiescent environments. Another possible source for the increased modification of the water masses is direct ventilation of the Atlantic-origin Water within or slightly offshore of the EGC (Våge et al. 2018). This would lead to a decrease in temperature of the Atlantic-origin Water but only a modest change in salinity. These two forms of modification are not opposing and both may well take place.

Despite the trend of decreasing Atlantic-origin Water temperature from north to south (Fig. 4a) the shelfbreak EGC transports both warm and cold Atlantic-origin Water along the entire east coast of Greenland. This corresponds well with our results from the Kögur mooring array which showed that warm and cold Atlantic-origin Water were transported by the shelfbreak branch (Fig. 3), although the temperature range was greatly reduced at the mooring transect. If the increased modification of the water masses south of 69°N is related to the bifurcation of the current, we would expect a signature of this in the kinematics of the EGC

system at Kögur. The mooring array covered both the shelfbreak EGC and the separated EGC and in the following section we analyze the two branches together and discuss their covariability.

5. Structure of the East Greenland Current branches at Kögur

We separated the Atlantic-origin Water in the shelfbreak EGC into a warm and a cold mode (Fig. 3b) and performed a composite analysis. At each time step the areas covered by warm and cold Atlantic-origin Water in the shelfbreak EGC were calculated from the gridded temperature field to quantify when and where the modes were present and their relative fractions of the overflow layer (Fig. 6a). The offshore limit of the shelfbreak EGC was set to KGA 8 (Harden et al. 2016; Håvik et al. 2017b). The amount of warm Atlantic-origin Water steadily increased from September through February (Fig. 6a). In March the warm mode nearly vanished before a slow increase took place toward summer. The presence of the cold mode was largely out of phase with the warm mode, however, the relationship was not linear since the amount of Atlantic-origin overflow Water varied with time (Fig. 6a). Other methods of identifying warm and cold modes, for example by the magnitude of the intermediate temperature maximum in vertical profiles extracted from the gridded product, yielded similar results. The corresponding transport of warm and cold mode waters revealed a persistent transport of the warm mode water throughout the year (Fig. 6b), although it has a limited presence (Fig. 6a). This corresponds to the transport maximum of the warm mode water in Fig. 3b.

To construct vertical sections of hydrographic properties and velocity we made composites of the periods when one mode dominated the other. A threshold value was chosen such that the difference between the area covered by each water mass had to exceed one standard deviation from the mean difference between the two types (marked by circles in Fig. 6). The analysis gave qualitatively similar results for other thresholds, but by choosing this value we included a sufficient number of time steps to create robust composites of current speed and hydrographic properties (176 and 131 members for the warm and cold modes, respectively).

The composite of the warm mode showed a layer with potential temperature $> 1^\circ\text{C}$ approximately between 300- and 700-m depth in the shelfbreak EGC (Fig. 7a). The warm core was accompanied by a high-salinity layer ($S > 34.92$, Fig. 7c) situated slightly deeper in the water column. Within the PSW a frontal zone with downsloping isopycnals toward Greenland supported a

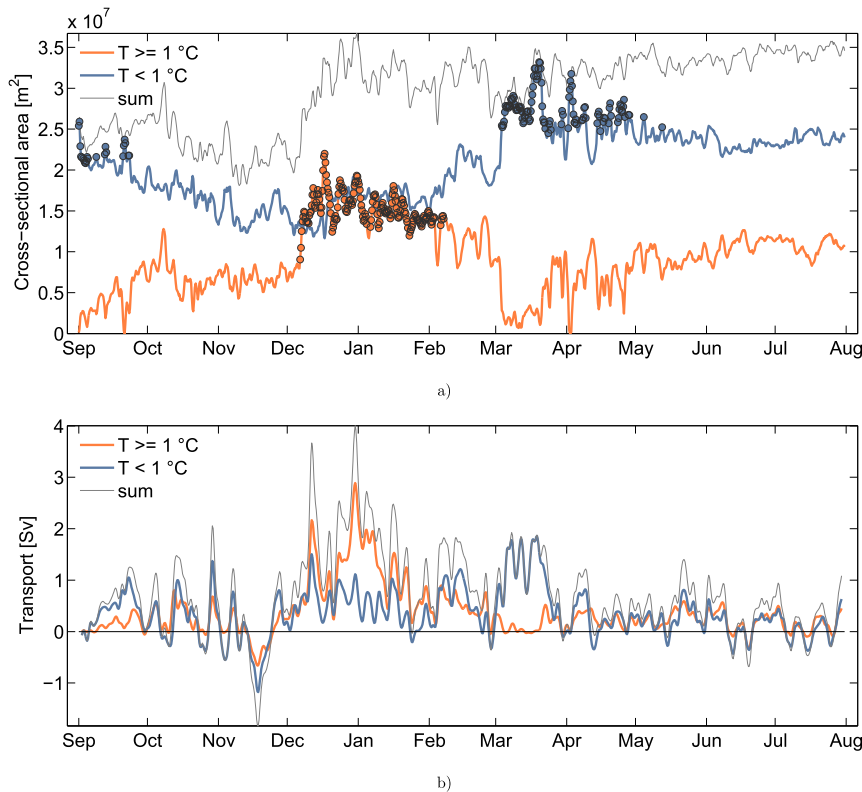


FIG. 6. (a) Area occupied by warm (orange) and cold (blue) Atlantic-origin Water in the shelfbreak EGC at the Kögur section from September 2011 to August 2012. The circles mark the times contributing to the composites presented in Fig. 7. The gray line represents the total area covered by Atlantic-origin Water in the shelfbreak EGC. (b) Transport of the warm (orange) and cold (blue) Atlantic-origin Water in the shelfbreak EGC throughout the year. The gray line represents the total transport of Atlantic-origin Water in the shelfbreak EGC. The data in (b) are low-pass filtered with a cutoff frequency of three days for better presentation.

strong shelfbreak current (Fig. 7e). The occurrence of warm Atlantic-origin Water and a strong shelfbreak current led to the relatively high transport of this water mass despite its limited presence (Fig. 3).

In the cold mode the warm water almost disappeared from the section and only a small area at around 300-m depth offshore of KGA 9 had temperatures $> 1^{\circ}\text{C}$ (Fig. 7b). The high-salinity layer was absent and no salinities above 34.92 were observed (Fig. 7d). In this case the surface layer was colder and fresher farther offshore and the front between the PSW and the warmer water masses to the east was shifted offshore toward KGA 7. In the vicinity of the Greenland shelf break the slope of the isopycnals in the surface layer was reduced compared to the warm mode, resulting in a wider, weaker, and shallower shelfbreak current (Fig. 7f).

Across the southeastern part of the Kögur transect, between approximately KGA 3 and KGA 6, the separated EGC and the NIJ flow into Denmark Strait (Harden et al. 2016). Equatorward flow was evident in

this region during both the warm and the cold modes but the exact configuration between the periods dominated by warm and cold modes was different. In the cold mode, the equatorward flow was surface-intensified close to KGA 6, indicating a pronounced separated EGC (Fig. 7f). The NIJ was located closer to Iceland and KGA 3, and characterized by a middepth intensification. In the warm mode the surface-intensification of the current was less pronounced and the intermediate current maximum close to KGA 4 associated with the NIJ was the strongest kinematic feature on the eastern end of the transect (Fig. 7e). These results indicate that the kinematic structure of the current branches is tightly coupled to the water masses that they carry, specifically to the properties of the Atlantic-origin Water.

When Våge et al. (2013) first identified the separated EGC they presented two hypotheses for the mechanism that causes the bifurcation. They suggested that negative wind stress curl across Blosseville basin would maintain a semipermanent anticyclonic gyre with its

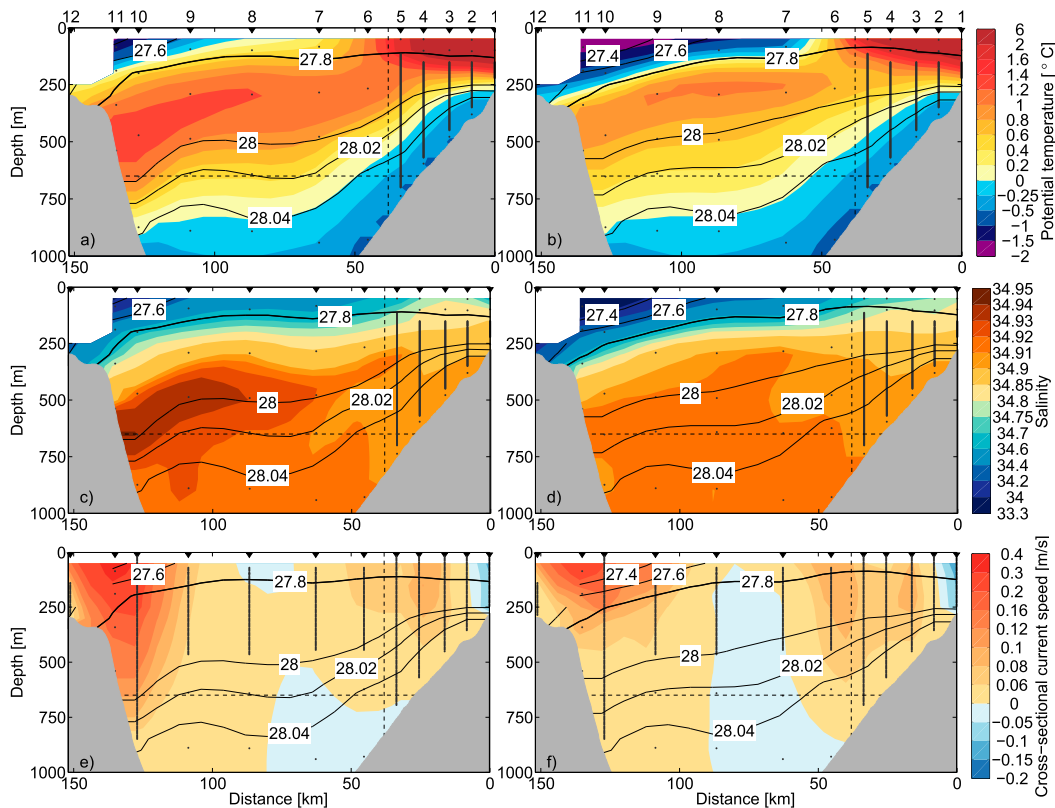


FIG. 7. Composite vertical sections across the entire Kögur array of (left) the warm mode and (right) the cold mode: (a),(b) potential temperature; (c),(d) salinity; and (e),(f) cross-sectional current speed. Positive current speeds are toward the southwest. On top of each section the mooring locations are indicated by the inverted triangles, and the measurement levels on each mooring are marked by black dots. A selection of isopycnals is contoured, and the upper limit of DSOw, the 27.8 kg m⁻³ isopycnal, is marked by the thick black contour. The horizontal dashed lines indicate the sill depth at Denmark Strait (650 m), and the vertical dashed lines mark the location where the orientation of the transect changes.

easternmost part being the separated current branch. This was elaborated upon and supported by [Harden et al. \(2016\)](#). The alternative hypothesis was based on results from numerical modeling, both with idealized and realistic bathymetry. This hypothesis suggested that the bifurcation is a result of baroclinic instabilities in the northern end of Blosseville basin that generate a train of eddies which coalesce along the base of the Iceland slope and form the separated EGC. Since the continental shelf near 69°N has a sharp bend to the west (close to the breakpoint in our trend analysis, [Fig. 5](#)), the dominant northerly wind is no longer parallel to the shelf at this point, and the onshore component of the Ekman transport does not support the surface front at the shelf break. Baroclinic instabilities were then found to erode the surface front and lead to the formation of the separated EGC.

Based on our results and a comparison to [Våge et al. \(2013\)](#), we hypothesize that the presence of cold and warm Atlantic-origin Water depends on the vigor of the

bifurcation at the northern end of Blosseville basin. The composite analysis suggests that this is directly connected to the resulting strength of the shelf break and separated branches of the EGC farther downstream. The hydrographic properties of the Atlantic-origin Water change more rapidly south of the bifurcation point ([Fig. 5](#)), indicating increased mixing. Following [Våge et al. \(2013\)](#) formation of eddies in this region may lead to an offshore shift of the cold and fresh surface layer and a consolidation of the separated EGC. This is reminiscent of the cold mode ([Figs. 7b,d,f](#)). The eddy activity led to a more vigorous mixing of the water masses and the overall temperature in the Atlantic-origin layer decreased. In the warm mode we found a weakened separated EGC, while a stronger shelfbreak EGC transported warmer and more saline Atlantic-origin Water ([Figs. 7a,c,e](#)). With a surface front close to the east Greenland shelf, this indicated that fewer eddies were shed from the current compared to the cold mode. Due to sea ice across the region of the mooring array

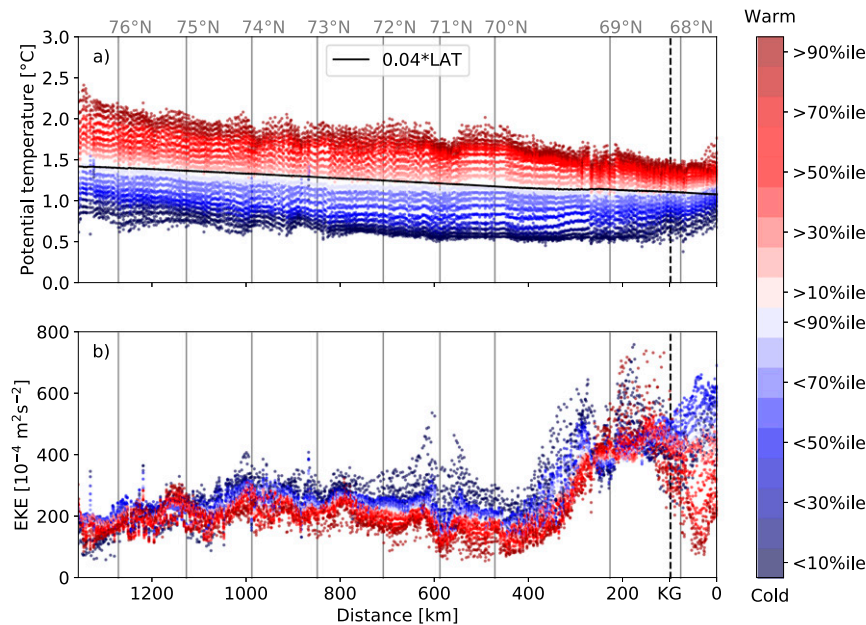


FIG. 8. (a) Average temperature of the Atlantic-origin Water along the shelfbreak EGC path computed for water warmer (red) and colder (blue) than a range of local percentiles (color bar), and (b) corresponding EKE. Larger distances correspond to higher latitudes, as shown by the vertical lines. The dashed vertical lines mark the latitude of the Kögrur section. The Atlantic-origin Water temperature was detected using the same criteria used for observations (cf. section 2b).

during winter we cannot directly evaluate our hypothesis against observations from satellite altimetry. However, we proceed with output of hydrography and velocity from the high-resolution numerical model to further elucidate the bifurcation of the EGC and the resulting warm and cold modes of the Atlantic-origin Water.

6. Eddy activity in East Greenland Current

In agreement with the observations (cf. section 4), the maximum temperature of the Atlantic-origin layer decreased from north to south in the model (Fig. 8a). The model showed a narrower temperature range and a weaker decrease (0.04°C per degree of latitude on average compared to 0.1°C per degree of latitude in the observations).

EKE varies both in time and space and we defined its temporal mean value along the path of the shelfbreak EGC as

$$\frac{1}{2}[(\bar{u} - u)^2 + (\bar{v} - v)^2],$$

where \bar{u} was the mean and u the instantaneous zonal current speed, and \bar{v} and v referred to the mean and instantaneous meridional current speeds, respectively. North of approximately 69.5°N the EKE in the

shelfbreak EGC was low compared to farther south (Fig. 8b). Although the cold mode was generally associated with enhanced eddy activity (blue dots), the two modes exhibited similar EKE values in the northern part. By contrast, there was a clear relationship between the core temperature of the Atlantic-origin Water and the strength of the eddy activity in the southern part of the shelfbreak EGC. Specifically, the two modes exhibited opposite behavior south of 68.5°N: the EKE associated with the cold (warm) mode increased (decreased) as the EGC approached Denmark Strait. This corroborates our hypothesis that formation of eddies plays a key role from the breakpoint (approximately located at 69°N) and southward, and that the cold mode is associated with stronger EKE than the warm mode.

To further investigate the relationship between the temperature modes and EKE we made model composites of cross-sectional current speed and EKE at times of warm and cold Atlantic-origin Water at Kögrur. We note that the average temperature of the Atlantic-origin Water at the latitude of the Kögrur transect was 1.1°C (Fig. 8a), similar to the threshold used for the composite analysis (Fig. 7). Thus, the periods contributing to the composites were detected in the same way as in the observations (cf. section 5). During warm conditions the shelfbreak EGC was the most pronounced circulation feature across the section (Fig. 9a), while the

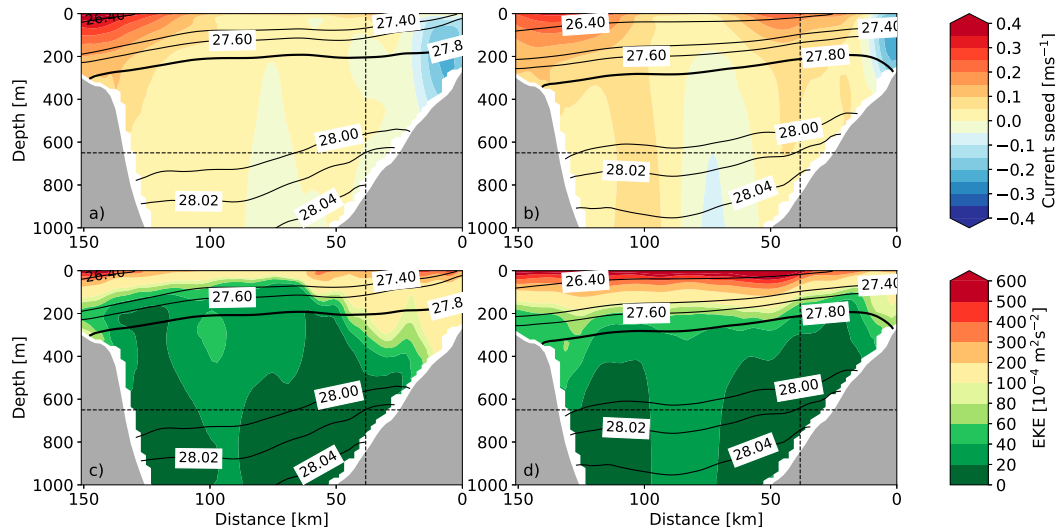


FIG. 9. Cross-sectional current speed at Kögur during (a) the warm mode and (b) the cold mode in the model. (c),(d) EKE during the warm and cold modes, respectively. Note the nonlinear color bar in (c) and (d). A selection of isopycnals is contoured in all panels, and the upper limit of DSOw, the 27.8 kg m^{-3} isopycnal, is marked by the thick black contour. The vertical dashed lines mark the location where the orientation of the transect changes.

separated branch was weak. The corresponding EKE was highest in the core of the shelfbreak current, but farther offshore the EKE was low (Fig. 9c). In the cold mode, on the other hand, the separated EGC was clearly visible in the composite vertical section (Fig. 9b). Increased EKE values were present across the entire Blosseville basin (Fig. 9d), with a maximum coinciding with the strongest flow in the separated EGC.

We summarize our findings with lateral maps of mean key surface (vertically averaged over 0–100 m) properties from the model (Fig. 10). The mean current speed in the upper 100 m indicated a strong shelfbreak EGC upstream of the Kögur transect (Fig. 10a) with an average flow which exceeded 0.4 m s^{-1} . Progressing southward in Blosseville basin the clear current core disintegrated and a broader region of enhanced current speed was evident on the east Greenland shelf and toward the Denmark Strait sill. There was no evidence of a distinct separated EGC in the mean, but as noted by Harden et al. (2016) this current branch is highly fluctuating both in time and space, hence a distinct flow path is not necessarily expected. The average surface salinity depicted the anticipated lateral distribution of water masses with fresh polar surface water on the shelf and more saline water masses offshore (Fig. 10b). North of the breakpoint the front between the two water masses was located close to the shelf break. In Blosseville basin, on the other hand, the front was less distinct and the freshwater masses were spreading east of the shelf break.

The enhanced eddy activity south of 69°N , required by our hypothesis to explain the difference in along-stream

temperature trends caused by enhanced mixing at the northern end of Blosseville basin, was clearly evident in the mean field of EKE in the model (Fig. 10c). The order of magnitude and location of enhanced EKE were consistent with estimates from satellite altimetry (Håvik et al. 2017b). South of approximately 68.2°N the EKE was also enhanced at the eastern end of Blosseville basin. This may be an indicator of the consolidation of the separated EGC as eddies coalesced along the base of the Iceland slope (Våge et al. 2013). We showed that in the observations the fresh polar water was shifted east during periods when the cold mode dominated (Fig. 7d), while the freshwater masses were mostly confined to the east Greenland shelf when the warm mode dominated (Fig. 7c). A correlation between EKE and surface salinity (Fig. 10d) revealed that high EKE was indeed associated with low salinities at the eastern end of Blosseville basin. On the other hand, low EKE, which we related to less formation of eddies in the shelfbreak EGC, was associated with high salinities. A particular strong correlation was found in an elongated band along the base of the Iceland slope (correlation ~ -0.7), where the separated EGC is hypothesized to form. To address the significance of the correlation coefficients, we performed two different significance tests. The slashes in Fig. 10d indicate correlation values that are not significant at the 5% level (p values < 0.05). The second method is based on Wilks (2016) and is more robust to the effects of spatial correlation. Wilks (2016) showed that, when the spatial correlation is moderate or strong, $\alpha_{\text{FDR}} = 2\alpha_{\text{global}}$ is the control level required to

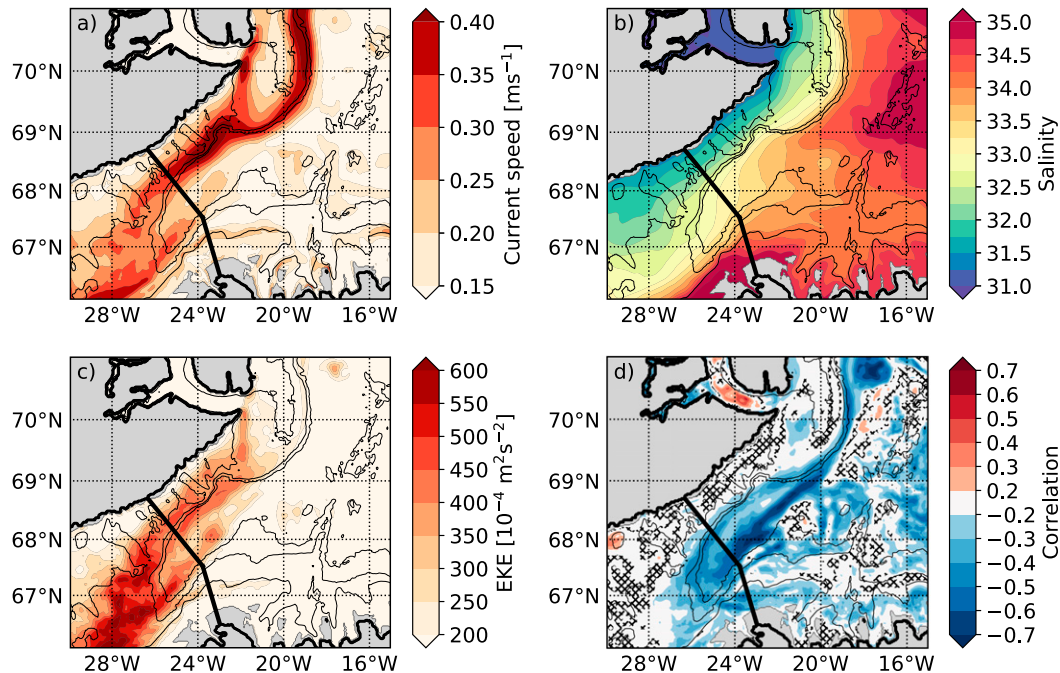


FIG. 10. Mean (a) current speed ($\sqrt{u^2 + v^2}$), (b) salinity, (c) EKE, and (d) Pearson correlation coefficient between salinity and EKE in the model over the upper 0–100 m. The black lines indicate the location of the Kögur transect. The gray contours are 300-, 700-, 1000-, and 2000-m isobaths from the model. Areas shallower than 100 m are masked gray. Hatched areas are not significant at the 5% level (p values < 0.05).

perform a solid false discovery rate (FDR) test. Thus, we chose $\alpha_{\text{FDR}} = 0.1$. The backslashes indicate correlation values that did not pass this test. About 85% of the grid points passed both test. With the model, we have now established the link between the EKE, the upper-ocean salinity, and the kinematic structure at Kögur, supporting the observations.

7. Discussion and conclusions

We have analyzed the properties of the Atlantic-origin Water in the EGC system using moored measurements and historical hydrographic profiles along the east coast of Greenland from Fram Strait to Denmark Strait. To support and extend the observational analysis we used output from a high-resolution numerical model. We showed that the temperature of the Atlantic-origin layer in the shelfbreak EGC decreased from Fram Strait to Denmark Strait and that an enhanced reduction was found south of 69°N at the northern end of Blossville basin. A similar decrease was found for salinity. Upstream of the breakpoint there was substantial variability from profile to profile within a range of approximately 1°–4°C. A couple of processes are likely responsible for setting this temperature range. Most importantly, it is not expected that the modification of the water is uniform neither temporally nor spatially. Some Atlantic-origin

Water may be advected relatively unperturbed in the shelfbreak current (Håvik et al. 2017a) whereas other parts are more strongly influenced by mixing with surrounding waters. A colder and less saline variant of Atlantic-origin Water exported in the shelfbreak EGC from the Arctic Ocean may be responsible for some of the cold Atlantic-origin Water profiles (Rudels et al. 2002). Additionally, Atlantic Water in Fram Strait exhibits a seasonal variability of 1°–2°C (Beszczynska-Möller et al. 2012), and this signal likely propagates downstream in the EGC. South of the breakpoint no water with a potential temperature $> 2.5^\circ\text{C}$ was observed and an increasing number of profiles showed a potential temperature maximum $< 1^\circ\text{C}$. This change in hydrographic properties and density of the Atlantic-origin layer between Fram Strait and Denmark Strait is contrary to the results of Mauritzen (1996), who found that the Atlantic-origin Water was advected relatively unperturbed in the EGC.

We hypothesize that the strong reduction south of the breakpoint is a result of enhanced mixing due to the bifurcation of the EGC at the northern end of Blossville basin. At Kögur we observed the downstream effects of the bifurcation. There we found that in periods a warm mode ($\theta > 1^\circ\text{C}$) of the Atlantic-origin Water was transported by the shelfbreak EGC, whereas the separated EGC on average transported a more modified version

with a lower temperature ($\theta < 1^\circ\text{C}$). Based on the mooring data we showed that at times of warm Atlantic-origin Water the shelfbreak EGC was stronger, whereas the separated current was weak. Oppositely, during periods dominated by the cold mode the shelfbreak current was weaker and the separated EGC correspondingly stronger (Fig. 7). The warm mode dominated during the winter months (DJF), whereas the cold mode was most prominent the rest of the year. At times almost no warm Atlantic-origin Water was present across the entire domain. With only one year of data we cannot conclude whether this is a seasonal signal or a coincidence, however, the seasonality of the Atlantic Water temperature in Fram Strait may add to this variability.

In addition to the more vigorous mixing of the intermediate Atlantic-origin Water south of 69°N , the cold and fresh surface layer is diverted offshore by the bifurcation process. This is important for the transport and distribution of freshwater (Våge et al. 2013) and it is evident that in the case of a strong separated current (Fig. 7f) the cold and fresh surface layer was diverted off the Greenland shelf (Fig. 7d). The model indicated that high EKE across Blosseville basin was associated with fresh surface water offshore of the shelf (Fig. 10d), and that eddies (presumably created by instabilities in the shelfbreak current) fluxed the surface water offshore. In the model, the total volume transport in the EGC system was similar in the two modes, but the relative contribution of the separated branch was larger during the cold mode. This supports the idea that the separated EGC results from a bifurcation of the shelfbreak EGC at the northern end of Blosseville basin.

The bifurcation process is hypothesized to take place due to a combination of bathymetry and wind forcing (Våge et al. 2013; Harden et al. 2016). In addition, we speculate that the vertical stability of the water column close to the northern end of the Blosseville basin can influence how susceptible the current is to baroclinic instability. This in turn depends on the core temperature of the Atlantic-origin Water. If the water at the breakpoint has a relatively high Atlantic-origin Water temperature the current is vertically less stable. This process may then lead to the erosion of the Atlantic-origin Water with the highest temperature through a release of baroclinic instabilities. Without knowledge of the advective time scale from the breakpoint to the Kögur transect the extent and importance of this process in determining the vigor of the bifurcation remains an open question.

Strass et al. (1993) concluded from a mooring deployed farther north in the EGC, at the latitude of the central Greenland Sea, that the conditions for baroclinic

instability were fulfilled during parts of the year. The exchange with the Greenland Sea would reduce the temperature and salinity maxima in the Atlantic-origin Water and they suggested that this modification may be important for the production of DSOW. Although the model indicated that cold water generally was associated with enhanced eddy activity, the relationship between the temperature of the Atlantic-origin Water and the intensity of the EKE became more pronounced south of approximately 69°N where the variability in EKE was higher. Specifically, we found that south of the breakpoint the EKE associated with the cold mode was twice as large as the EKE in the warm mode.

Våge et al. (2018) found that Atlantic-origin Water was reventilated offshore of the shelfbreak EGC. This was possible due to a recent retreat of the ice edge, in combination with strong atmospheric fluxes just offshore of the ice edge and an onshore Ekman transport. If the sea ice continues to retreat toward Greenland this reventilation of the Atlantic-origin Water may take place directly within the core of the current and lead to a further modification of this water mass. Both the increased modification due to the bifurcation of the current and the direct modification of the Atlantic-origin Water in the shelfbreak EGC (Våge et al. 2018) represent possible mechanisms which can alter the density of the overflow water directly within the East Greenland Current. This may, in turn, influence the density of the overflow through Denmark Strait and the contribution from the Nordic Seas to the deep circulation in the North Atlantic.

Acknowledgments. Support for this work was provided by the Research Council of Norway under Grant Agreement 231647 (LH and KV) and the Bergen Research Foundation under Grant BFS2016REK01 (KV). MA and TH are supported by NSF Awards OCE-1433448, OCE-1633124. The mooring data can be obtained from <http://kogur.whoj.edu>. We thank GWK Moore for valuable insights regarding breakpoints in data series.

REFERENCES

- Almansi, M., T. W. N. Haine, R. S. Pickart, M. G. Magaldi, R. Gelderloos, and D. Mastropole, 2017: High-frequency variability in the circulation and hydrography of the Denmark Strait Overflow from a high-resolution numerical model. *J. Phys. Oceanogr.*, **47**, 2999–3013, <https://doi.org/10.1175/JPO-D-17-0129.1>.
- Bamber, J., M. Van Den Broeke, J. Ettema, J. Lenaerts, and E. Rignot, 2012: Recent large increases in freshwater fluxes from Greenland into the North Atlantic. *Geophys. Res. Lett.*, **39**, L19501, <https://doi.org/10.1029/2012GL052552>.

- Behrens, E., K. Våge, B. Harden, A. Biastoch, and C. W. Böning, 2017: Composition and variability of the Denmark Strait Overflow Water in a high-resolution numerical model hindcast simulation. *J. Geophys. Res. Oceans*, **122**, 2830–2846, <https://doi.org/10.1002/2016JC012158>.
- Beszczynska-Möller, A., E. Fahrbach, U. Schauer, and E. Hansen, 2012: Variability in Atlantic water temperature and transport at the entrance to the Arctic Ocean, 1997–2010. *ICES J. Mar. Sci.*, **69**, 852–863, <https://doi.org/10.1093/icesjms/fss056>.
- Bourke, R. H., R. G. Paquette, and R. F. Blythe, 1992: The Jan Mayen Current of the Greenland Sea. *J. Geophys. Res.*, **97**, 7241–7250, <https://doi.org/10.1029/92JC00150>.
- Brakstad, A. D., K. Våge, L. Håvik, and G. Moore, 2019: Water mass transformation in the Greenland Sea during the period 1986–2016. *J. Phys. Oceanogr.*, **49**, 121–140, <https://doi.org/10.1175/JPO-D-17-0273.1>.
- Bromwich, D., and Coauthors, 2018: The Arctic System Reanalysis, version 2. *Bull. Amer. Meteor. Soc.*, **99**, 805–828, <https://doi.org/10.1175/BAMS-D-16-0215.1>.
- Buch, E., S.-A. Malmberg, and S. S. Kristmannsson, 1996: Arctic Ocean deep water masses in the western Iceland Sea. *J. Geophys. Res.*, **101**, 11 965–11 973, <https://doi.org/10.1029/95JC03869>.
- de Steur, L., E. Hansen, C. Mauritzen, A. Beszczynska-Möller, and E. Fahrbach, 2014: Impact of recirculation on the East Greenland Current in Fram Strait: Results from moored current meter measurements between 1997 and 2009. *Deep-Sea Res. I*, **92**, 26–40, <https://doi.org/10.1016/j.dsr.2014.05.018>.
- , R. S. Pickart, A. Macrander, K. Våge, B. Harden, S. Jónsson, S. Østerhus, and H. Valdimarsson, 2017: Liquid freshwater transport estimates from the East Greenland Current based on continuous measurements north of Denmark Strait. *J. Geophys. Res. Oceans*, **122**, 93–109, <https://doi.org/10.1002/2016JC012106>.
- Dee, D. P., and Coauthors, 2011: The ERA-Interim reanalysis: Configuration and performance of the data assimilation system. *Quart. J. Roy. Meteor. Soc.*, **137**, 553–597, <https://doi.org/10.1002/qj.828>.
- Dickson, R. R., and J. Brown, 1994: The production of North Atlantic Deep Water: Sources, rates, and pathways. *J. Geophys. Res. Oceans*, **99**, 12 319–12 341, <https://doi.org/10.1029/94JC00530>.
- Eldevik, T., J. E. Ø. Nilsen, D. Iovino, K. A. Olsson, A. B. Sandø, and H. Drange, 2009: Observed sources and variability of Nordic seas overflow. *Nat. Geosci.*, **2**, 406–410, <https://doi.org/10.1038/ngeo518>.
- Haine, T. W. N., S. Zhang, G. Moore, and I. Renfrew, 2009: On the impact of high-resolution, high-frequency meteorological forcing on Denmark Strait ocean circulation. *Quart. J. Roy. Meteor. Soc.*, **135**, 2067–2085, <https://doi.org/10.1002/qj.505>.
- , and Coauthors, 2015: Arctic freshwater export: Status, mechanisms, and prospects. *Global Planet. Change*, **125**, 13–35, <https://doi.org/10.1016/j.gloplacha.2014.11.013>.
- Hansen, B., K. M. Húsgrud Larsen, H. Hátún, and S. Østerhus, 2016: A stable Faroe Bank Channel overflow 1995–2015. *Ocean Sci.*, **12**, 1205–1220, <https://doi.org/10.5194/os-12-1205-2016>.
- Harden, B. E., and Coauthors, 2016: Upstream sources of the Denmark Strait Overflow: Observations from a high-resolution mooring array. *Deep-Sea Res. I*, **112**, 94–112, <https://doi.org/10.1016/j.dsr.2016.02.007>.
- Hattermann, T., P. E. Isachsen, W.-J. von Appen, J. Albrechtsen, and A. Sundfjord, 2016: Eddy-driven recirculation of Atlantic Water in Fram Strait. *Geophys. Res. Lett.*, **43**, 3406–3414, <https://doi.org/10.1002/2016GL068323>.
- Håvik, L., R. S. Pickart, K. Våge, D. Torres, A. M. Thurnherr, A. Beszczynska-Möller, W. Walczowski, and W.-J. von Appen, 2017a: Evolution of the East Greenland Current from Fram Strait to Denmark Strait: Synoptic measurements from summer 2012. *J. Geophys. Res. Oceans*, **122**, 1974–1994, <https://doi.org/10.1002/2016JC012228>.
- , K. Våge, R. S. Pickart, B. Harden, W.-J. von Appen, S. Jónsson, and S. Østerhus, 2017b: Structure and variability of the shelfbreak East Greenland Current north of Denmark Strait. *J. Phys. Oceanogr.*, **47**, 2631–2646, <https://doi.org/10.1175/JPO-D-17-0062.1>.
- Jeansson, E., S. Jutterström, B. Rudels, L. G. Anderson, K. A. Olsson, E. P. Jones, W. M. Smethie, and J. H. Swift, 2008: Sources to the East Greenland Current and its contribution to the Denmark Strait Overflow. *Prog. Oceanogr.*, **78**, 12–28, <https://doi.org/10.1016/j.pocean.2007.08.031>.
- Jochumsen, K., M. Moritz, N. Nunes, D. Quadfasel, K. M. H. Larsen, B. Hansen, H. Valdimarsson, and S. Jónsson, 2017: Revised transport estimates of the Denmark Strait overflow. *J. Geophys. Res. Oceans*, **122**, 3434–3450, <https://doi.org/10.1002/2017JC012803>.
- Jónsson, S., 1992: Sources of fresh water in the Iceland Sea and the mechanisms governing its interannual variability. *ICES Mar. Sci. Symp.*, **195**, 62–67.
- , 1999: The circulation in the northern part of the Denmark Strait and its variability. ICES Rep. CM1999/L:06, 9 pp.
- Latarius, K., and D. Quadfasel, 2016: Water mass transformation in the deep basins of the Nordic Seas: Analyses of heat and freshwater budgets. *Deep-Sea Res. I*, **114**, 23–42, <https://doi.org/10.1016/j.dsr.2016.04.012>.
- Losch, M., D. Menemenlis, J. M. Campin, P. Heimbach, and C. Hill, 2010: On the formulation of sea-ice models. Part 1: Effects of different solver implementations and parameterizations. *Ocean Modell.*, **33**, 129–144, <https://doi.org/10.1016/j.ocemod.2009.12.008>.
- Lozier, M. S., and Coauthors, 2017: Overturning in the Subpolar North Atlantic Program: A new international ocean observing system. *Bull. Amer. Meteor. Soc.*, **98** (4), 737–752, <https://doi.org/10.1175/BAMS-D-16-0057.1>.
- Macrander, A., H. Valdimarsson, and S. Jónsson, 2014: Improved transport estimate of the East Icelandic Current 2002–2012. *J. Geophys. Res. Oceans*, **119**, 3407–3424, <https://doi.org/10.1002/2013JC009517>.
- Marshall, J., A. Adcroft, C. Hill, L. Perelman, and C. Heisey, 1997: A finite-volume, incompressible Navier Stokes model for studies of the ocean on parallel computers. *J. Geophys. Res.*, **102**, 5753–5766, <https://doi.org/10.1029/96JC02775>.
- Mastropole, D., R. S. Pickart, H. Valdimarsson, K. Våge, K. Jochumsen, and J. Girton, 2017: On the hydrography of Denmark Strait. *J. Geophys. Res. Oceans*, **122**, 306–321, <https://doi.org/10.1002/2016JC012007>.
- Mauritzen, C., 1996: Production of dense overflow waters feeding the North Atlantic across the Greenland-Scotland Ridge. Part 1: Evidence for a revised circulation scheme. *Deep-Sea Res. I*, **43**, 769–806, [https://doi.org/10.1016/0967-0637\(96\)00037-4](https://doi.org/10.1016/0967-0637(96)00037-4).
- Moore, G., D. H. Bromwich, A. B. Wilson, I. Renfrew, and L. Bai, 2016: Arctic System Reanalysis improvements in topographically forced winds near Greenland. *Quart. J. Roy. Meteor. Soc.*, **142**, 2033–2045, <https://doi.org/10.1002/qj.2798>.
- Noël, B., W. J. van de Berg, H. Machguth, S. Lhermitte, I. Howat, X. Fettweis, and M. R. van den Broeke, 2016: A daily, 1 km

- resolution data set of downscaled Greenland ice sheet surface mass balance (1958–2015). *Cryosphere*, **10**, 2361–2377, <https://doi.org/10.5194/tc-10-2361-2016>.
- Østerhus, S., and Coauthors, 2019: Arctic Mediterranean Exchanges: A consistent volume budget and trends in transports from two decades of observations. *Ocean Sci.*, **15**, 379–399, <https://doi.org/10.5194/os-15-379-2019>.
- Rudels, B., E. Fahrbach, J. Meincke, G. Budëus, and P. Eriksson, 2002: The East Greenland Current and its contribution to the Denmark Strait overflow. *ICES J. Mar. Sci.*, **59**, 1133–1154, <https://doi.org/10.1006/jmsc.2002.1284>.
- , G. Björk, J. Nilsson, P. Winsor, I. Lake, and C. Nohr, 2005: The interaction between waters from the Arctic Ocean and the Nordic Seas north of Fram Strait and along the East Greenland Current: Results from the Arctic Ocean-02 Oden expedition. *J. Mar. Syst.*, **55**, 1–30, <https://doi.org/10.1016/j.jmarsys.2004.06.008>.
- Sakov, P., F. Counillon, L. Bertino, K. A. Lister, P. R. Oke, and A. Korabely, 2012: TOPAZ4: An ocean-sea ice data assimilation system for the North Atlantic and Arctic. *Ocean Sci.*, **8**, 633–656, <https://doi.org/10.5194/os-8-633-2012>.
- Strass, V. H., E. Fahrbach, U. Schauer, and L. Sellmann, 1993: Formation of Denmark Strait overflow water by mixing in the East Greenland Current. *J. Geophys. Res.*, **98**, 6907–6919, <https://doi.org/10.1029/92JC02732>.
- Våge, K., R. S. Pickart, M. A. Spall, H. Valdimarsson, S. Jónsson, D. J. Torres, S. Østerhus, and T. Eldevik, 2011: Significant role of the North Icelandic Jet in the formation of Denmark Strait overflow water. *Nat. Geosci.*, **4**, 723–727, <https://doi.org/10.1038/ngeo1234>.
- , —, —, G. Moore, H. Valdimarsson, D. J. Torres, S. Y. Erofeeva, and J. E. Ø. Nilsen, 2013: Revised circulation scheme north of the Denmark Strait. *Deep-Sea Res. I*, **79**, 20–39, <https://doi.org/10.1016/j.dsr.2013.05.007>.
- , G. Moore, S. Jónsson, and H. Valdimarsson, 2015: Water mass transformation in the Iceland Sea. *Deep-Sea Res. I*, **101**, 98–109, <https://doi.org/10.1016/j.dsr.2015.04.001>.
- , L. Papritz, L. Håvik, M. Spall, and G. Moore, 2018: Ocean convection linked to the recent ice edge retreat along east Greenland. *Nat. Commun.*, **9**, 1287, <https://doi.org/10.1038/s41467-018-03468-6>.
- von Appen, W.-J., U. Schauer, T. Hattermann, and A. Beszczynska-Möller, 2016: Seasonal cycle of mesoscale instability of the West Spitsbergen Current. *J. Phys. Oceanogr.*, **46**, 1231–1254, <https://doi.org/10.1175/JPO-D-15-0184.1>.
- , D. Mastropole, R. S. Pickart, H. Valdimarsson, S. Jónsson, and J. B. Girton, 2017: On the nature of the mesoscale variability in Denmark Strait. *J. Phys. Oceanogr.*, **47**, 567–582, <https://doi.org/10.1175/JPO-D-16-0127.1>.
- Wilks, D. S., 2016: “The stippling shows statistically significant grid points”: How research results are routinely overstated and overinterpreted, and what to do about it. *Bull. Amer. Meteor. Soc.*, **97**, 2263–2273, <https://doi.org/10.1175/BAMS-D-15-00267.1>.